Article

Not peer-reviewed version

A Multifunctionalized Potyvirus-Derived Nanoparticle That Targets and Internalizes into Cancer Cells

Daniel A. Truchado , María Juárez-Molina , Sara Rincón , Lucía Zurita , Jaime Tomé-Amat , Corina Lorz , Fernando Ponz *

Posted Date: 7 February 2024

doi: 10.20944/preprints202402.0392.v1

Keywords: turnip mosaic virus; VLP; protein A; Z-domain; cetuximab; squamous cell carcinoma; viral nanoparticles

Article

A multifunctionalized Potyvirus-Derived Nanoparticle That Targets and Internalizes into Cancer Cells

Daniel A. Truchado [1], María Juárez-Molina [1,2], Sara Rincón [1], Lucía Zurita [1], Jaime Tomé-Amat [1], Corina Lorz [3,4,5] and Fernando Ponz [1]

[1] Centro de Biotecnología y Genómica de Plantas (CBGP), Instituto Nacional de Investigación y Tecnología Agraria y Alimentaria (INIA-CSIC), Universidad Politécnica de Madrid (UPM). Pozuelo de Alarcón. Spain
[2] Present address: Instituto de Biología Molecular y Celular de Plantas (IBMCP; UPV-CSIC). C/ de l'Enginyer Fausto Elio, s/n, Algirós. València. Spain
[3] Unidad de Innovación Biomédica, CIEMAT, Ave Complutense 40, Madrid, Spain
[4] Instituto de Investigación Sanitaria Hospital 12 de Octubre (imas12), Avenida de Córdoba s/n, Madrid, Spain
[5] Centro de Investigación Biomédica en Red de Cáncer (CIBERONC), Avenida de Monforte de Lemos 3-5, Madrid, Spain
* Correspondence: fponz@inia.csic.es

Abstract: Plant viral nanoparticles (VNPs) are attractive to researchers in nanomedicine due to their safety, easy production, resistance, and straightforward functionalization. In this paper, we developed and successfully purified a VNP derived from turnip mosaic virus (TuMV), a well-known plant pathogen, that exhibits high affinity for immunoglobulins G (IgG) thanks to its functionalization with the Z domain from staphylococcal protein A via gene fusion. We selected cetuximab as a model IgG to prove the versatility of this novel TuMV VNP by developing a fluorescent nanoplatform to mark tumoral cells of the line Cal33, from tongue squamous cell carcinoma. We observed that the fluorescent VNP-cetuximab bound selectively to Cal33 and were internalized by confocal microscopy, revealing the potential of this nanotool in cancer research.

Keywords: turnip mosaic virus; VLP; protein A; Z-domain; cetuximab; squamous cell carcinoma; viral nanoparticles

1. Introduction

The use of viral nanoparticles (VNPs) in cancer research has become increasingly common in recent years due to their biocompatibility, self-assembly, wide range of shapes and their easily modifiable composition [1,2]. Plant VNPs are especially noteworthy as they are not infective for humans and are easily produced by molecular farming [3]. Plant-made VNPs include virions, which are infective to plants, and virus-like particles (VLPs), without any infectious ability as they are formed by self-assembled capsid proteins (CPs). Elongated and rod-shaped VNPs are especially attractive for cancer research as they have shown better tumor homing than other alternative shapes [4].

Turnip mosaic virus (TuMV) is one example of an elongated, flexuous plant virus whose VNPs have been used to develop a great number of nanotools with applications in different areas, including cancer research [5]. In that case, TuMV virions that were chemically functionalized with epigallocatechin gallate (EGCG) showed good tumor homing and antiproliferative effect in Cal33 cells, which derived from tongue squamous cell carcinoma (SCC) [6]. In this study, however, we aimed at developing a TuMV-derived VLP with high antibody affinity to target specifically tumor cells from SCC. Overexpression of the epidermal growth factor receptor (EGFR) is common in this type of cancer, what makes it a good target for developing new therapeutic agents [7–9]. One of such therapeutic agents is cetuximab, a mouse/human chimeric monoclonal antibody that binds EGFR with higher affinity than its natural ligands transforming growth factor alfa (TGF-α) and epidermal

 doi:10.20944/preprints202402.0392.v1

growth factor (EGF), preventing them from interacting with the receptor [10]. It also promotes the internalization of EGFR [11]. Cetuximab has been successfully used in the treatment of SCC, as well as other human cancers with an EGFR overexpression such as the colorectal type [12]. Therefore, binding cetuximab to TuMV VLPs should allow their binding to SCC cells with high affinity and, eventually, internalize them into the cell.

In order to bind cetuximab to the surface of TuMV VLPs, the fusion of a protein sequence providing high affinity for antibodies to the CP was required. Protein A from *Staphylococcus aureus* is a well-known protein with 5 homologous immunoglobulin-binding domains (A-E) of 56-61 amino acids. These domains interact with the fragment crystallizable (Fc) of immunoglobulins G (IgG) of a wide variety of mammals without affecting their antigen-binding ability. Protein A has been frequently used to immobilize antibodies to a solid surface, especially for antibody purification [13]. In this study, we used the Z-domain to functionalize TuMV VLPs via gene fusion and provide them with affinity for IgGs. This Z-domain is a synthetic sequence of 58 amino acids, derived from the domain B of staphylococcal Protein A, which shows more stability than the original and presents a structure of 3 antiparallel helixes [14,15]. Functionalization of elongated VNPs with IgG-binding domains of Protein A is not new, and it has also been performed in other plant viruses [16–18]. However, unlike the other plant-made VNPs, TuMV VLPs are twice as long (around 720 nm) and offer more binding sites to the IgGs as their capsid protein is represented approximately 2,000 copies in each particle.

Functionalized TuMV VLPs-cetuximab were found to interact with EGFR-overexpressing Cal33 cells, derived from a tongue SCC and their specific binding was assessed compared to VLPs-Z domain alone. The objective of this paper is to show a novel approach to selectively functionalize TuMV VLPs by binding the antibody of interest to their surface. As a proof of concept, we also want to demonstrate the potential of this VLP-Z domain as a platform to develop a nanocarrier targeted to tumor cells overexpressing EGFR.

2. Results

2.1. VLP purification and cetuximab functionalization check

The correct purification of the VLP-Z domain was confirmed by SDS-PAGE and Western blot, where a single band of the expected molecular weight for the recombinant protein CP-Z domain (40.9 kDa; Figure 1) was observed (Figure 2A). This result was also supported by ELISA (Figure 2B). Micrographs obtained through transmission electron microscopy (TEM) revealed the correct assembly of the VLPs (Figure 2C).

Regarding the functionalization with cetuximab, the results of the indirect ELISA showed that VLPs-Z domain were able to successfully bind cetuximab when we coated the plates with them (Figure 3).

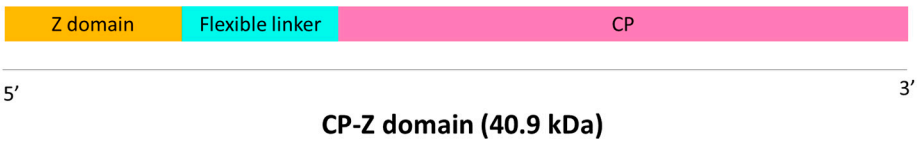

Figure 1. Schematic representation of the synthetic gene designed in this study. A flexible linker (GGGGSGGGGSGGGGS) was added to physically separate the two parts of the fusion protein to avoid steric hinderance. CP: TuMV capsid protein.

Preprints.org (www.preprints.org) | NOT PEER-REVIEWED | Posted: 7 February 2024 doi:10.20944/preprints202402.0392.v1

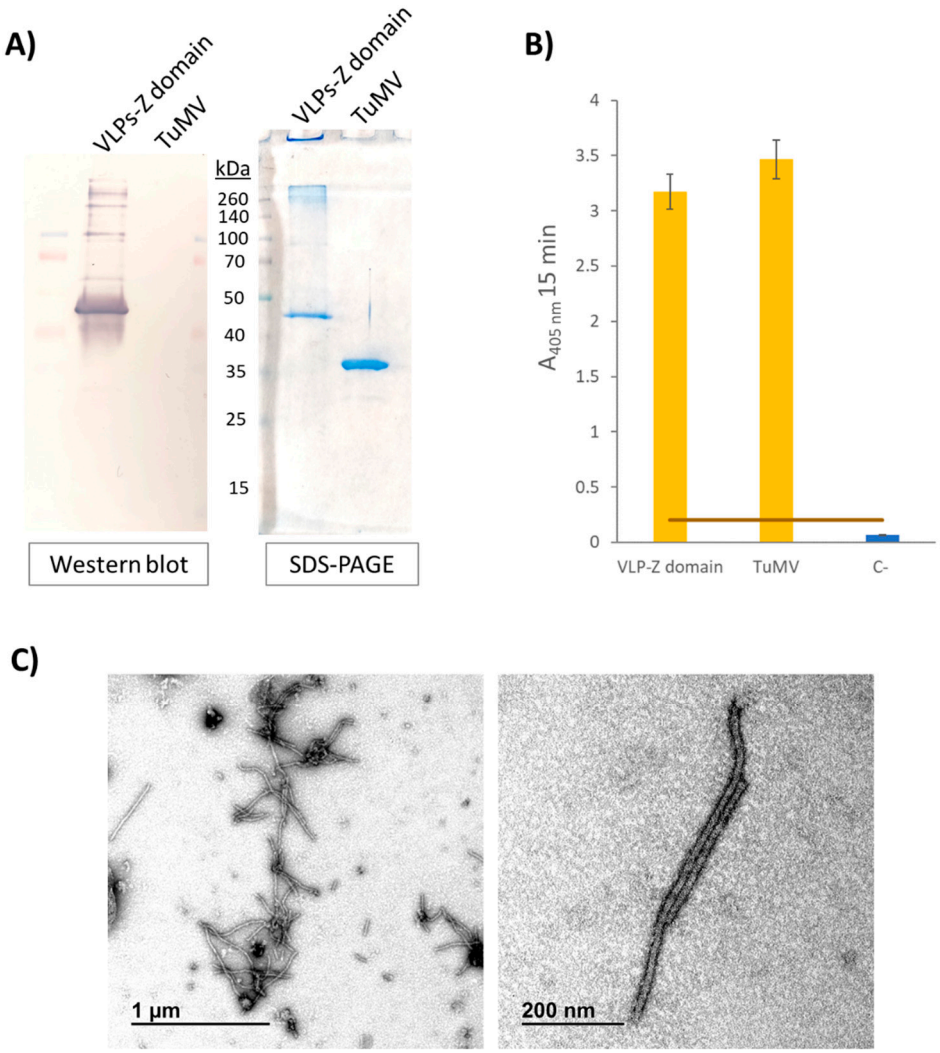

Figure 2. A) Western blot results using anti-potyvirus as the primary antibody and stained SDS-PAGE polyacrylamide gel with the same samples. Approximate molecular weight of the different bands of the marker (Spectra™ Multicolor Broad Range Protein Ladder, Fisher Scientific, USA) are highlighted. Positive control (TuMV) could not be observed in the Western blot likely due to the high affinity for IgG of the VLP-Z domain construct. **B)** Results of the indirect ELISA carried out to chek for the presence of the CP in the purified VLPs-Z domain. The error bars show the 95 % confidence interval for the absorbance values. The orange bar represent the threshold to consider a positive result set at three times the value of the negative control. **C)** Micrographs of the purified VLPs-Z domain obtained by TEM. VLP: virus-like particles; TuMV: turnip mosaic virus.

 doi:10.20944/preprints202402.0392.v1

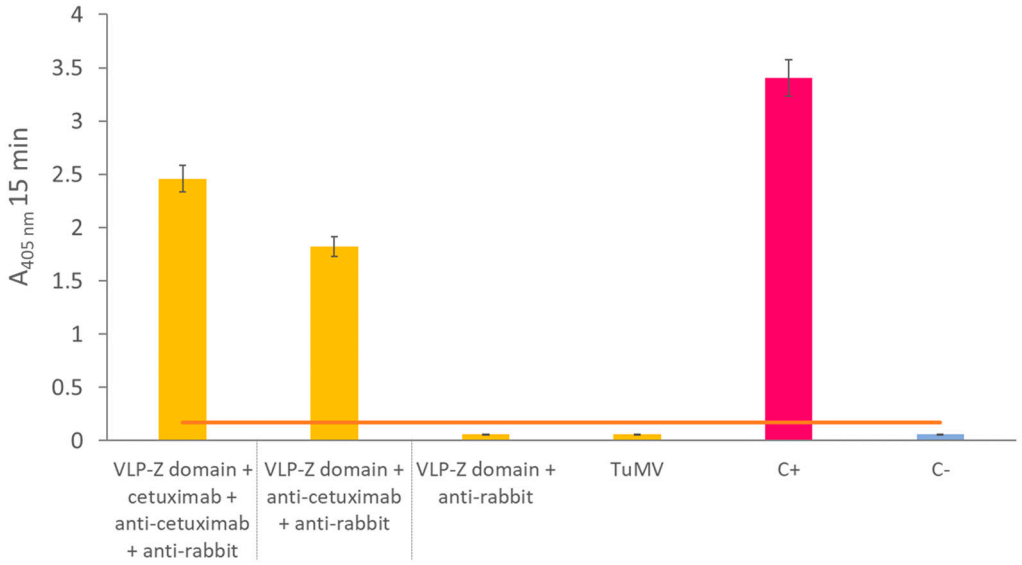

Figure 3. Results of the indirect ELISA in which the ability of VLPs-Z domain to bind cetuximab was tested. The error bars show the 95 % confidence interval for the absorbance values. The orange bar represent the threshold to consider a positive result set at three times the value of the negative control. C+: positive control consisting of a coating step with 10 µg of free cetuximab. C-: negative control where no coating step was performed. VLP: virus-like particles; TuMV: turnip mosaic virus**.**

2.2. Triple functionalization of VLP-Z domain with cetuximab and Cy5.5

We observed different results depending on wether cetuximab was conjugated before (functionalization A) or after the fluorescent dye Cy5.5 (see Figure 7). The high fluorescence values of the VLP-Cy5.5 and the VLP of the functionalization A (cetuximab first) showed that the fluorescent dye was correctly linked to the constructs and was detectable at the same time. However, the fluorescence detected in the case of the VLP from the functionalization B (Cy5.5 first) was very low indicating that conjugating cetuximab after chemically linking the Cy5.5 dye hampered the detection of the fluorescence (Figure 4A), possibly due to a quenching effect.

The indirect ELISA revealed that, despite the successful binding to the Z-domain of the VLP, cetuximab could not be detected clearly when Cy5.5 was linked afterwards (functionalization A), which may be explained by the fact that the dye probably masked the epitope recognized by the primary anti-cetuximab antibody. On the other hand, Cy5.5 conjugation does not hinder the detection of CP by the anti-potyvirus antibody. However, when cetuximab was present, the CP epitope was not recognized (Figure 4B).

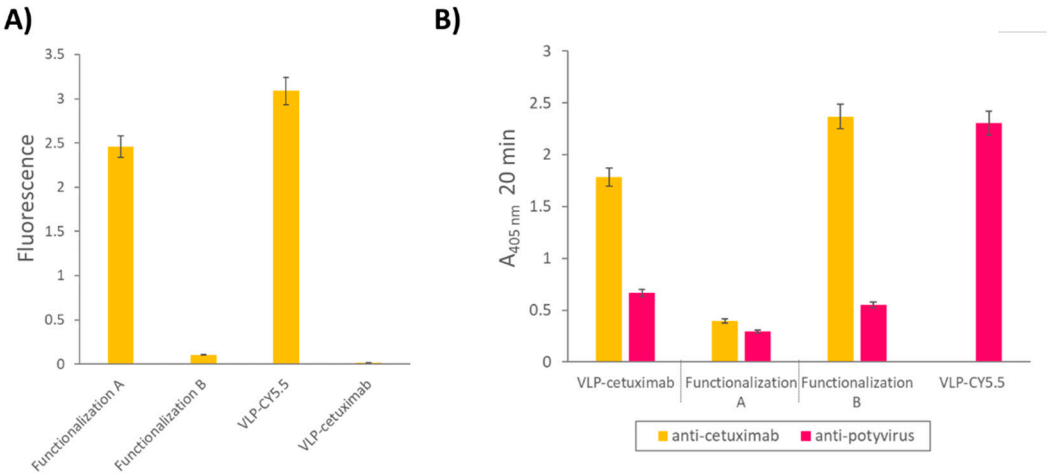

 doi:10.20944/preprints202402.0392.v1

Figure 4. A) Fluorescence values of the different functionalized VLPs obtained for the excitation and emission expectra corresponding to the Cy5.5 dye. **B)** ELISA results using anti-cetuximab and anti-potyvirus as primary antibodies with the different functionalized VLPs. VLP-Cy5.5 was analyzed only with anti-potyvirus. The error bars show the 95 % confidence interval for the absorbance values. Functionalization A: double-functionalized VLP in which cetuximab was conjugated first and Cy5.5 afterwards. Functionalization B: double-functionalized VLP in which Cy5.5 was conjugated first and cetuximab afterwards. VLP: virus-like particle.

2.3. Cell viability assay

The results obtained from the colorimetric assay revealed that none of the constructs affected cell viability as any of them showed a significant difference with the positive control of Cal33 cells without stumulus (Figure S1, Table S1).

2.4. Flow cytometry

Results from the flow cytometry assays showed that VLPs-cetuximab-Cy5.5 from the functionalization A (cetuximab first) bound selectively to Cal33 cells (overexpressing EGFR) but not to THP1 (without EGFR overexpression). However, in the case of VLPs from functionalization B, the dye Cy5.5 could not be detected (Figure 5). All negative controls resulted as expected (Figure S2)

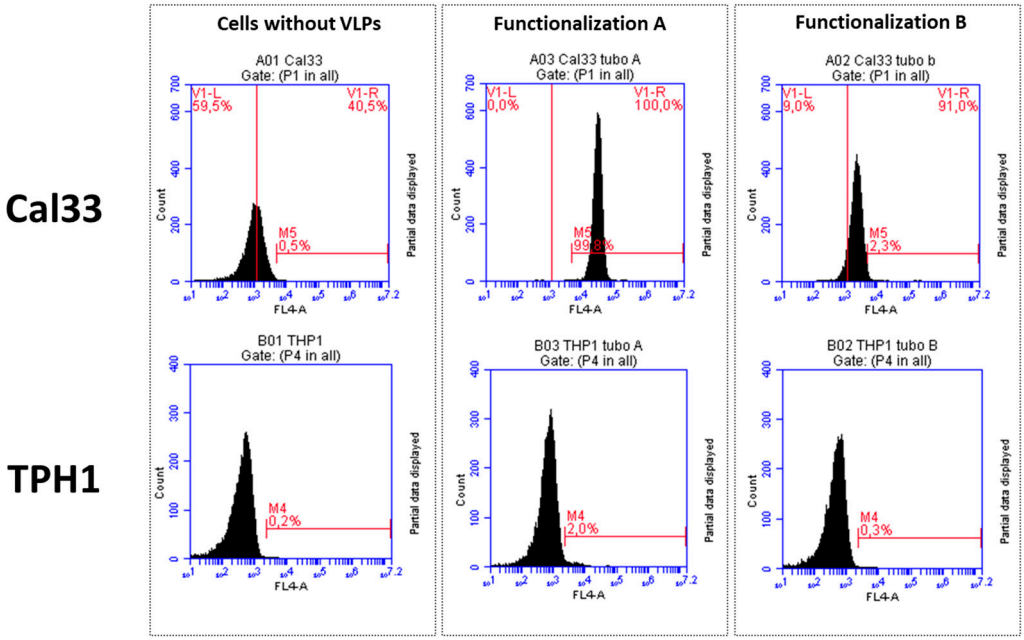

Figure 5. Flow cytometry analysis of VLP-cetuximab-Cy5.5 binding to Cal33 (EFGR+) and THP1 (EGFR-) cells. Upper row shows Cal33 cells in the absence of VLPs (left) and in the presence of VLPs (Functionalization A, middle), (Functionalization B, right). Lower row shows equivalent samples in THP1 cells.

2.5. Confocal microscopy

Given the results obtained with flow cytometry, we discarded VLPs from functionalization B (Cy5.5 first) and carried out the experiment for the confocal microscopy using only VLP-cetuximab-Cy5.5 from functionalization A (cetuximab first). As a first experiment, we checked that free cetuximab marked with Cy5.5 bound to Cal33 cells as expected under the same conditions as VLPs (Figure S2). Images from confocal microscopy of Cal33 cells incubated with the two fluorescent VLPs constructs revealed that VLPs-cetuximab-Cy5.5 bound to a greater extent to the cells than VLPs-Cy5.5

 doi:10.20944/preprints202402.0392.v1

(without cetuximab). Furthermore, VLPs-cetuximab-Cy5.5 seem to enter the cells after 24 h of incubation and tend to accumulate in a perinuclear location (Figure 6).

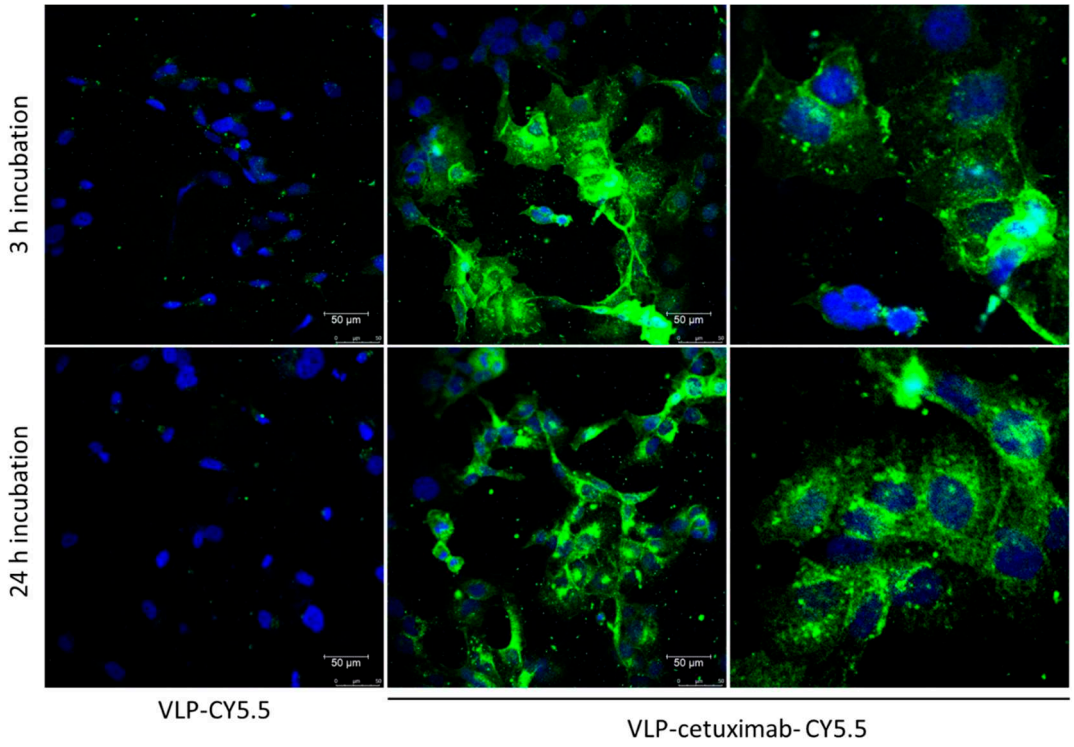

Figure 6. Representative images of Cal33 cells marked with fluorescent TuMV VLPs (either VLP-Cy5.5 alone or VLP-cetuximab-Cy5.5; in green) after an incubation of 3 h (upper panels) and 24 h (lower panels). Cell nuclei were dyed with DAPI (blue). One-micrometer-thick slices were made in the area equidistant between the apical and basal poles of the cells. .

3. Discussion

In this paper we demonstrate that TuMV VLPs can be successfully functionalized with the Z-domain derived from Protein A, resulting in a highly versatile nanoplatform that can readily bind IgGs. As an example, their triple functionalization using cetuximab and Cy5.5 results in a fluorescent nanoparticle targeted to tumor cells with great interest in cancer research. Also, it was the first time that functionalized TuMV VLPs were successfully purified, solving for this construct one of the major problems we faced with other TuMV VLPs [19].

The use of plant VNPs in nanomedicine has increased in the last years due to the advantages they offer. Plant VNP CPs self-assemble and are biosafe, biocompatible and present a well-known structure that allows a straightforward modification of their compositions through chemical and genetic manipulation [20,21]. One of the fields were plant VNPs have shown great potential is in cancer research [22], where several examples of plant VNPs in cancer imaging and theranostics can be found. Elongated plant VNPs have been used in cancer research before, mainly as nanocarriers of drugs such as doxorubicin or cisplatin [23,24]. Viruses with high aspect ratios such as potato virus X, tobacco mosaic virus or TuMV tend to improve drug delivery as they are retained and accumulated in tumor areas more than their icosahedral counterparts [25]. In our group, we showed that TuMV virions present good tumor homing in vivo, as expected given their elongated capsid [6]. In the present study, we were able to functionalize TuMV VLPs with antibodies targeted specifically towards EGFR, what would increase their performance in a tumor environment as they will have not only good tumor homing but also high affinity attachment to cells overexpressing this receptor. This could be observed both in the different fluorescent marking of Cal33 when using VLPs-Cy5.5 alone or VLP-cetuximab-Cy5.5 in confocal microscopy and in the different marking of Cal33

 doi:10.20944/preprints202402.0392.v1

(overexpressing EGFR) and THP1 (without EGFR) in flow cytometry. Moreover, we observed fluorescent VLPs inside Cal33 cells after 24 h of incubation in confocal microscopy, indicating that they have the potential to be used as nanocarriers and internalize drugs coating the VLP surface. TuMV VNPs stand out among all other plant-made VNPs because they are the longest, offering more space to be functionalized also with an antitumoral of interest. These characteristics are of great interest for cancer types where EGFR overexpression occurs, such as head and neck squamous carcinomas, glioblastomas or lung and breast cancer [26–28].

One of the main applications of the fluorescent TuMV VLP we developed would be cancer theranostics, especially optical imaging. Despite we used the fluorescence of Cy5.5 to confirm the affinity of the construct for Cal33 cells, the nanotool itself could be employed to mark tumoral cells with high sensitivity. Other VNPs have been used for this purpose instead of synthetic nanoparticles due to two main reasons: less side effects given their short circulation and retention times and their easily modifiable composition for improved targeting [2,29]. Different plant VNPs have been used for tumor imaging so far, with special emphasis on those derived from cowpea mosaic virus (CPMV) [30–32]. However, TuMV VLPs are elongated and flexuous, with all the advantages already mentioned in comparison with icosahedral viruses.

The main drawback we faced in this study was the absence of fluorescence in the construct where Cy5.5. was conjugated first and then cetuximab was added to the VLP. This may be explained by the different size of cetuximab (152 kDa) compared to Cy5.5 (1.3 kDa) and their relative position. Cetuximab would be densely coating the VLP, covering the fluorescence of the Cy5.5 conjugated first and making it undetectable in the different analyses. By conjugating Cy5.5 after cetuximab, not only did we overcome this problem but also the binding of cetuximab to EGFR was not affected.

Apart from cancer research, a nanoplatform based on VNPs with high affinity for IgGs has other multiple applications in the field of antigen sensing. Two other potyviruses (zucchini yellow mosaic virus and tobacco etch virus) functionalized with nanobodies have been recently developed through genome engineering, revealing the attractiveness of this group of plant viruses for antibody presentation [33]. Also, our VLPs-Z domain go a step further as they can readily bind other IgGs of interest and they can be double-functionlalized with other compounds through chemical conjugation, giving them a huge versatility as a novel nanoplatform.

In conclusion, we report the development and successful purification of a TuMV VLP with high affinity for IgGs. As a proof of concept, we used cetuximab as a model IgG to develop a fluorescent VLPs specifically targeted to cancer cells overexpressing EGFR, resulting in an interesting nanoplatform for cancer theranostics.

4. Materials and Methods

4.1. Cloning in expression vectors and agroinfiltration

First, a synthetic gene containing the sequence of the Z domain of *Staphylococcus aureus* protein A fused to the CP of TuMV was designed. The Z domain was fused to the N-terminus of the CP as this is the part exposed to the solvent, and both sequences were separated by a flexible linker to avoid steric hindrances (Figure 1). This synthetic gene was designed and ordered from GeneArt (Thermo Fisher Scientific, Regensburg, Germany). This gene construct was cloned in the pEAQ-HT-DEST1 vector [34] and *Escherichia coli* top 10 cells (Thermo Fisher Scientific, Germany) to finally transform cells of *Agrobacterium tumefaciens* (LBA4404 strains) for transient expression in *Nicotiana benthamiana*. Agroinfiltration took place using a needless syringe, following a protocol described elsewhere [19].

4.2. Purification of VLP-Z domain

Agroinfiltrated leaves were harvested at 6 dpi. Then, eVLP-Z domain were purified following a protocol described before for TuMV virions [35], with some modifications. Briefly, leaves were ground in 0.5 M potassium phosphate buffer, pH 7.5 (100 mL buffer per 50 g of leaves) using a blender. Then, the product was filtered through a masher and a gauze, and chloroform was added to the liquid phase (50 mL per 50 g of leaves). After stirring for 10 min at 4 °C, the sample was

 doi:10.20944/preprints202402.0392.v1

centrifuged at 500 × g for 10 min at 4 °C to separate the different phases. Then, the aqueous upper phase was filtered through Miracloth filter (Merck Millipore, Germany) and centrifuged at 5000 × g for 10 min at 4 °C. The supernatant was filtered through Miracloth filter (Merck Millipore, Germany) and NaCl and PEG were added to a final concentration of 4 and 6 % (w/v) respectively. After stirring for 90 min at 4 °C, the sample was centrifuged at 12,000 × g for 10 min at 4 °C. The supernatant was discarded, and the pellet was resuspended in 0.5 M potassium phosphate buffer, pH 7.5 and 0.01 M EDTA pH 8.0 by stirring at 4 °C for 48 h. The suspension was then centrifuged at 80,000 × g for 2 h at 4 °C. The supernatant was discarded, and the pellet was resuspended in 0.25 M potassium phosphate buffer, pH 7.5, 0.01 M EDTA by stirring at 4 °C for 5 days. Then, the suspension was subjected to an isopycnic centrifugation using CsCl at 150,000 × g for 18 h at 4 °C in a fixed-angle rotor without brake. Finally, the band containing the VLP-Z domain was obtained by puncturing with a syringe.

4.3. Characterization of purified VLPs-Z domain

Characterization of purified VLPs was performed by SDS-PAGE, Western blot and ELISA. Purified VLPs were subjected to a SDS-PAGE in a 12 % polyacrilamide gel with a stacking gel of 4 % (Bio-Rad, USA). Half of the gel was transferred to a PVDF membrane (Amersham™ Hybond™ P 0.45 PVDF, Cytiva, Spain) to carry out a Western blot while the other half was stained with Imperial™ Protein Stain (Thermo Scientific, USA) following manufacturer's instructions. The membrane for Western blot was blocked with 2 % skimmed milk in PBS overnight. The detection of the recombinant protein CP-Z domain (40.9 kDa) was carried out by an incubation with a 1:200 dilution of the primary monoclonal antibody anti-POTY (Agdia, USA) followed by a second incubation with a 1:500 dilution of the secondary antibody anti-mouse conjugated to alkaline phosphatase (Agdia, USA). Alkaline phosphatase activity was detected using 1-Step™ NBT/BCIP (Thermo Scientific, USA). Finally, we confirmed the detection of the VLPs-Z domain through an indirect ELISA. We coated high binding plates (Fisher Scientific, USA) with 0.5 µg/well of VLPs-Z domain (or TuMV virions in the case of the positive control) in a final volume of 200 µL of 50 mM sodium carbonate buffer, pH 9.6. After 45 min at 37 °C, plates were washed 3 times with PBS-Tween and blocked with BSA 0.2 % in 50 mM sodium carbonate buffer, pH 9.6 during 45 min at 37 °C. After the blocking step, plates were washed again with PBS-Tween 3 times. As the primary antibody, we used a 1:200 dilution of anti-POTY (Agdia, USA) and, as the secondary antibody, we used a 1:500 dilution of anti-mouse conjugated to alkaline phosphatase (Agdia, USA).

To confirm the correct assembly of VLPs-Z domain, we observed them by transmission electron microscopy (TEM). To do so, a 400-mesh copper-carbon-coated electron microscopy grid was floated with 10 µL of the purified VLPs for 10 min. Then, the grid was washed with five drops of distilled H_2O for 5 min each. Eventually, the grid was stained with 2 % (w/v) uranyl acetate for 3 min and examined on a transmission electron microscope (JEM JEOL 1400, Tokyo, Japan) in an external service (TEM, ICTS-CNME, Madrid, Spain).

4.4. VLP-Z domain functionalization with cetuximab

To create a nanotool based on the TuMV VLPs that binds specifically tumor cells with overexpressed EGFR, we checked whether they could bind cetuximab through the Z domains that we fused to the CPs. To that end, we carried out an ELISA in which we coated high binding plates (Fisher Scientific, USA) with 0.5 µg/well of VLPs- Z domain. After an overnight incubation at 4 °C, plates were washed 3 times with PBS-Tween and blocked with BSA 0.2 % in 50 mM sodium carbonate buffer, pH 9.6 during 1 h at 37 °C. Then, they were incubated with 10 µg/well of cetuximab for 1h at 37 °C. After washing three times with PBS-Tween, plates were incubated with a 1:1000 dilution of the primary antibody anti-cetuximab (R&D Systems, USA) for 1 h at 37 °C. Finally, after other 3 washes with PBS-Tween, plates were incubated with a 1:2000 dilution of the secondary antibody anti-rabbit conjugated to alkaline phosphatase (Invitrogen). In all cases, antibodies (including cetuximab) were diluted in PBS, 0.05 % Tween 20, 2 % PVP-40, 2 mg/mL BSA. We observed alkaline phosphatase activity using nitrophenylphosphate as a substrate and measuring the absorbance of the wells at 405

 doi:10.20944/preprints202402.0392.v1

nm (SPECTROstar Nano®; BMG Labtech, Germany). A negative control with no coating step was added. The positive control consisted of a well coated with 10 µg of free cetuximab.

As the VLPs-Z domain presented high affinity for IgGs, we added two extra negative controls to this ELISA to discard false positives due to the binding of the Fc region of the primary and secondary antibodies to the Z domain that might remain free in the VLP. For these controls, we coated with 0.5 µg/well of VLP-Z domain in a final volume of 200 µL of 50 mM sodium carbonate buffer, pH 9.6. Then, one of the negative controls was incubated with anti-cetuximab as the primary antibody (without previously adding cetuximab) and anti-rabbit conjugated to alkaline phosphatase as the secondary antibody. The other negative control was incubated only with the secondary antibody anti-rabbit conjugated to alkaline phosphatase. Also, to discard that the affinity for IgG is not due to the TuMV CP itself, we added another negative control where we coated with 0.5 µg/well of free purified TuMV virions which were incubated with the primary and secondary antibodies detecting cetuximab.

4.5. Triple functionalization of VLP-Z domain with cetuximab and Cy5.5

Apart from the ability of the VLPs to bind tumor cells, we wanted them to be easily traceable by confocal microscopy, so we double-functionalized them with cetuximab and the fluorescent dye Cy5.5 in a second experiment. As we did not know a priori which combination would be most efficient (cetuximab first and then Cy5.5 or the other way round), we carried out in parallel both options named functionalization A (cetuximab first) and B (Cy5.5 first; Figure 7). For the functionalization with the monoclonal antibody, we mixed 32 µg of purified VLP-Z domain (with and without previously linked Cy5.5) with 325 µg of cetuximab (Erbitux®, Merck Europe B.V., Netherlands) in a final volume of 800 µL of HEPES 10 mM. Thus, cetuximab was 50 × molar excess in relation to TuMV CP. The mixture was left in agitation overnight at 4 °C. The excess of Cetuximab was removed by centrifuging the mixture at 100000 × g for 4 h at 4 °C. The pellet containing the functionalized VLPs, was resuspended in 800 µL of HEPES 10 mM. On the other hand, the functionalization with the fluorescent dye took place mixing 32 µg of purified VLP-Z domain (with and without previously linked cetuximab) with 3 × molar excess of Amersham™ Cy5.5 mono NHS ester (GE Healthcare, UK) in a final volume of 800 µL of HEPES 10 mM. This way, the fluorescent dye should coat the surface of the VLPs through bioconjugation to lysine residues exposed to the solvent [36]. The mixture was left overnight in agitation at 4 °C protected from the light. The excess of Cy5.5 was removed by centrifugal filters (Amicon ® Ultra – 0,5 mL Centrifugal Units 3 kDa, Merck Millipore, Germany). An extra sample, only with VLP-Z domain and Cy5.5 (without cetuximab) was added as a negative control for the subsequent analysis. All samples were resuspended in a final volume of 800 µL 10 mM HEPES.

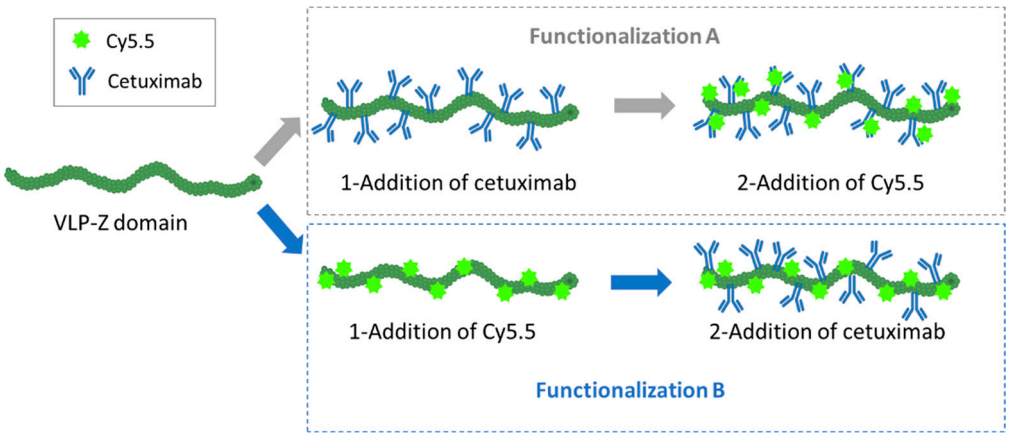

Figure 7. Representation of the two alternative ways through which VLP-Z domain were double-functionalized with cetuximab and Cy5.5 in this study.

 doi:10.20944/preprints202402.0392.v1

Once the VLPs were triple-functionalized, we checked for the correct conjugation of both Cy5.5 and cetuximab. For Cy5.5, fluorescence of the samples was measured (excitation = 683 nm; emission = 703 nm) using a Varioskan™ LUX multimode microplate reader (Thermo Scientific, Germany). In this analysis, we also included the construct with VLP-Cy5.5 alone. For cetuximab, we carried out an indirect ELISA to check for its presence in the samples. We coated high binding plates (Fisher Scientific, USA) with 0.5 µg/well of VLP-cetuximab-Cy5.5 from functionalizations A and B, and VLP-cetuximab without Cy5.5 in a final volume of 200 µL of 50 mM sodium carbonate buffer, pH 9.6. After 45 min at 37 °C, plates were washed 3 times with PBS-Tween and blocked with BSA 0.2 % in 50 mM sodium carbonate buffer, pH 9.6 during 45 min at 37 °C. After the blocking step, we used a 1:1000 dilution of the primary antibody anti-cetuximab (R&D Systems, USA) and a 1:2000 dilution of the secondary antibody anti-rabbit conjugated to alkaline phosphatase (Invitrogen). Both antibodies were diluted in PBS, 0.05 % Tween 20, 2 % PVP-40, 2 mg/mL BSA; incubations took place for 1 h at 37 °C and plates were washed 3 times with PBS-Tween after every incubation. We observed alkaline phosphatase activity using nitrophenylphosphate as a substrate and measuring the absorbance of the wells at 405 nm (SPECTROstar Nano®; BMG Labtech, Germany). The same samples were analyzed in another indirect ELISA using anti-potyvirus to check for the presence of the VLP following the protocol mentioned before. In this ELISA, we also included the construct with VLP-Cy5.5 alone.

4.6. Cell viability assay

In order to discard that VLP (either functionalized or not) were toxic for tumor cells, cell viability was determined through a colorimetric method based on the bioreduction of a tetrazolium salt (MTS) to an intensely colored formazan. Cal33 cells were plated (around 5000 cells/well) in 96-well plates. After 24 h, they were treated with decreasing concentrations of the different constructs (both VLPs-cetuximab-Cy5.5, free non-functionalized VLPs, free cetuximab and free Cy5.5), ranging from 0.01 µg/µL to 0.0012 µg/µL, in a final volume of 100 µL of Dulbecco's Modified Eagle's Medium (DMEM, Gibco, Thermo Fisher Scientific, Germany). Cells with the constructs were incubated for other 24 h. After this, 20 µL MTS Cell Titer 96®AQueous One Solution (Promega, Thermo Fisher Scientific, USA) was added to each well and plates were read after incubating them for 2 h at 37 °C. Each experiment was performed in triplicate.

4.7. Flow cytometry

To check the specific interaction between VLPs-cetuximab-Cy5.5, we carried out a flow cytometry assay using two different cell lines: Cal33 (from squamous cell carcinoma, overexpressing EGFR) and THP1 (monocytes that do not express EGFR). Approximately 50,000 cells per experiment were incubated with 0.01 µg/mL of VLP-cetuximab-Cy5.5 (functionalization A and B) for 40 min at RT. We used a BD Accuri™ C6 Plus Personal Flow Cytometer (BD Biosciences; USA). We used near red laser light as background noise and far red laser to check for the presence of Cy5.5.

4.8. Confocal microscopy

Cal33 cells were seeded on round glass covers in a 24-well plate (approximately 300,000 cells/well) in Dulbecco's Modified Eagle's Medium (DMEM, Gibco, Thermo Fisher Scientific, Germany) and were incubated for 24 h at 37 °C. In half of the wells, 1 µg of each construct was added, and cells were incubated for 3h at 37 °C. After this, the medium with the construct was aspirated, cells washed, and changed for new Dulbecco's Modified Eagle's Medium (DMEM, Gibco, Thermo Fisher Scientific, Germany). Cells were incubated for other 24 h before preparing them for microscopy. In the other half of the wells, the medium was aspired and changed after 24 h, and 1 µg of each construct was added 3h before preparing them for microscopy, time during which they were incubated at 37 °C.

All Cal33 cells were washed 3 times with PBS and stained with DAPI. After washing 3 times with PBS, cells were fixed with 4 % paraformaldehyde and glass covers were mounted with

ProLong™ Gold (Thermo Fisher Scientific, USA) following manufacturer´s instructions. Micrographs were obtained using a fluorescence confocal microscope Leica TSC-SP8 (LAS X software).

Supplementary Materials: The following supporting information can be downloaded at the website of this paper posted on Preprints.org. Figure S1; Table S1 and Figure S2.

Author Contributions: Conceptualization, F.P. and C.L.; methodology, D.A.T., M.J., S.R., J.T., C.L. and F.P.; formal analysis, D.A.T., M.J., S.R., J.T., C.L. and F.P.; investigation, D.A.T., M.J., S.R., J.T.; writing—original draft preparation, D.A.T. and F.P..; writing—review and editing, D.A.T., M.J., S.R., J.T., C.L. and F.P.; funding acquisition, F.P. All authors have read and agreed to the published version of the manuscript."

Funding: This work was conceived as transversal to efforts experimentally aimed to TuMV nanobiotechnological functionalizations. Consequently, it has benefited from different grants obtained along the years. These are P2018/BAA-4574, COV20/00114, and PanGreen-CM from the Comunidad de Madrid; RTA2015-00017-00-00 from INIA; and ARIMNet-2 618127, an ERANet project. DAT was supported by a Margarita Salas postdoctoral grant funded by the Spanish Ministry of Universities and UCM (CT31/21). SR was funded by a contract under grant P2018/BAA-4574 from the Comunidad de Madrid. The CBGP was granted 'Severo Ochoa' Distinctions of Excellence by the Spanish Ministry of Science and Innovation (SEV- 2016-0672 and CEX2020-000999-S).

Acknowledgments: the authors want to thank Alba Rubio for the preparation of the samples for TEM visualization.

Conflicts of Interest: authors declare no conflicts of interest.

References

1. Jeevanandam, J.; Barhoum, A.; Chan, Y.S.; Dufresne, A.; Danquah, M.K. Review on Nanoparticles and Nanostructured Materials: History, Sources, Toxicity and Regulations. *Beilstein J. Nanotechnol.* **2018**, *9*, 1050–1074, doi:10.3762/bjnano.9.98.
2. Chung, Y.H.; Cai, H.; Steinmetz, N.F. Viral Nanoparticles for Drug Delivery, Imaging, Immunotherapy, and Theranostic Applications. *Adv. Drug Deliv. Rev.* **2020**, *156*, 214–235, doi:10.1016/j.addr.2020.06.024.
3. Rybicki, E.P. Plant Molecular Farming of Virus-like Nanoparticles as Vaccines and Reagents. *Wiley Interdiscip. Rev. Nanomedicine Nanobiotechnology* **2020**, *12*, doi:10.1002/wnan.1587.
4. Shukla, S.; Hu, H.; Cai, H.; Chan, S.-K.; Boone, C.E.; Beiss, V.; Chariou, P.L.; Steinmetz, N.F. Annual Review of Virology Plant Viruses and Bacteriophage-Based Reagents for Diagnosis and Therapy. *Annu. Rev. Virol.* **2020**, *7*, 559–587, doi:10.1146/annurev-virology-010720.
5. Truchado, D.A.; Rincón, S.; Zurita, L.; Ponz, F. Turnip Mosaic Virus Nanoparticles: A Versatile Tool in Biotechnology. In *Tools & Techniques of Plant Molecular Farming. Concepts and Strategies in Plant Sciences*; Kole, C., Chaurasia, A., Hefferon, K.L.P.J., Eds.; Springer: Singapore, 2023; pp. 235–249.
6. Velázquez-Lam, E.; Tome-Amat, J.; Segrelles, C.; Yuste-Calvo, C.; Asensio, S.; Peral, J.; Ponz, F.; Lorz, C. Antitumor Applications of Polyphenol-Conjugated Turnip Mosaic Virus-Derived Nanoparticles. *Nanomedicine* **2022**, 999–1012, doi:https://doi.org/10.2217/nnm-2022-0067.
7. Hanawa, M.; Suzuki, S.; Dobashi, Y.; Yamane, T.; Kono, K.; Enomoto, N.; Ooi, A. EGFR Protein Overexpression and Gene Amplification in Squamous Cell Carcinomas of the Esophagus. *Int. J. Cancer* **2006**, *118*, 1173–1180, doi:10.1002/ijc.21454.
8. Ryott, M.; Wangsa, D.; Heselmeyer-Haddad, K.; Lindholm, J.; Elmberger, G.; Auer, G.; Lundqvist, E.Å.; Ried, T.; Munck-Wikland, E. EGFR Protein Overexpression and Gene Copy Number Increases in Oral Tongue Squamous Cell Carcinoma. *Eur. J. Cancer* **2009**, *45*, 1700–1708, doi:10.1016/j.ejca.2009.02.027.
9. Uribe, P.; Gonzalez, S. Epidermal Growth Factor Receptor (EGFR) and Squamous Cell Carcinoma of the Skin: Molecular Bases for EGFR-Targeted Therapy. *Pathol. Res. Pract.* **2011**, *207*, 337–342, doi:10.1016/j.prp.2011.03.002.
10. Baselga, J. The EGFR as a Target for Anticancer Therapy-Focus on Cetuximab. *Eur. J. Cancer* **2001**, *37*, 16–22.
11. Sunada, H.; Magunt, B.E.; Mendelsohn, J.; Macleod, C.L. Monoclonal Antibody against Epidermal Growth Factor Receptor Is Internalized without Stimulating Receptor Phosphorylation (Phosphotyrosine/Percoll Gradient/Epidermoid Carcinoma Cell). *Cell Biol.* **1986**, *83*, 3825–3829.
12. Bou-Assaly, W.; Mukherji, S. Cetuximab (Erbitux). *Am. J. Neuroradiol.* **2010**, *31*, 626–627, doi:10.3174/ajnr.A2054.

13. Rigi, G.; Ghaedmohammadi, S.; Ahmadian, G. A Comprehensive Review on Staphylococcal Protein A (SpA): Its Production and Applications. *Biotechnol. Appl. Biochem.* **2019**, *66*, 454–464, doi:10.1002/bab.1742.
14. Nilsson, B.; Moks, T.; Jansson, B.; Abrahmsen, L.; Elmblad, A.; Holmgren, E.; Henrichson, C.; Jones, T.A.; Uhlen, M. *A Synthetic IgG-Binding Domain Based on Staphylococcal Protein A*; 1987; Vol. 1;.
15. Myrhammar, A.; Rosik, D.; Karlström, A.E. Photocontrolled Reversible Binding between the Protein A-Derived Z Domain and Immunoglobulin G. *Bioconjug. Chem.* **2020**, *31*, 622–630, doi:10.1021/acs.bioconjchem.9b00786.
16. Wendlandt, T.; Koch, C.; Britz, B.; Liedek, A.; Schmidt, N.; Werner, S.; Gleba, Y.; Vahidpour, F.; Welden, M.; Poghossian, A.; et al. Facile Purification and Use of Tobamoviral Nanocarriers for Antibody-Mediated Display of a Two-Enzyme System. *Viruses* **2023**, *15*, 1951, doi:10.3390/v15091951.
17. Werner, S.; Marillonnet, S.; Hause, G.; Klimyuk, V.; Gleba, Y. Immunoabsorbent Nanoparticles Based on a Tobamovirus Displaying Protein A. *Proc. Natl. Acad. Sci.* **2006**, *103*, 17678–17683.
18. Kalnciema, I.; Balke, I.; Skrastina, D.; Ose, V.; Zeltins, A. Potato Virus M-like Nanoparticles: Construction and Characterization. *Mol. Biotechnol.* **2015**, *57*, 982–992, doi:10.1007/s12033-015-9891-0.
19. Truchado, D.A.; Rincón, S.; Zurita, L.; Sánchez, F.; Ponz, F. Isopeptide Bonding *in Planta* Allows Functionalization of Elongated Flexuous Proteinaceous Viral Nanoparticles, Including Non-Viable Constructs by Other Means. *Viruses* **2023**, *15*, 375, doi:10.3390/v15020375.
20. Czapar, A.E.; Steinmetz, N.F. Plant Viruses and Bacteriophages for Delivery in Medicine and Biotechnology. *Curr. Opin. Chem. Biol.* **2017**, *38*, 108–116, doi:10.1016/j.cbpa.2017.03.013.
21. Eiben, S.; Koch, C.; Altintoprak, K.; Southan, A.; Tovar, G.; Laschat, S.; Weiss, I.M.; Wege, C. Plant Virus-Based Materials for Biomedical Applications: Trends and Prospects. *Adv. Drug Deliv. Rev.* **2019**, *145*, 96–118, doi:10.1016/j.addr.2018.08.011.
22. Azizi, M.; Shahgolzari, M.; Fathi-Karkan, S.; Ghasemi, M.; Samadian, H. Multifunctional Plant Virus Nanoparticles: An Emerging Strategy for Therapy of Cancer. *Wiley Interdiscip. Rev. Nanomedicine Nanobiotechnology* **2023**, *15*, doi:10.1002/wnan.1872.
23. Le, D.H.T.; Lee, K.L.; Shukla, S.; Commandeur, U.; Steinmetz, N.F. Potato Virus X, a Filamentous Plant Viral Nanoparticle for Doxorubicin Delivery in Cancer Therapy. *Nanoscale* **2017**, *9*, 2348–2357, doi:10.1039/c6nr09099k.
24. Zhang, W.; Yang, S.; Shan, T.; Hou, R.; Liu, Z.; Li, W.; Guo, L.; Wang, Y.; Chen, P.; Wang, X.; et al. Virome Comparisons in Wild-Diseased and Healthy Captive Giant Pandas. *Microbiome* **2017**, *5*, 90, doi:10.1186/s40168-017-0308-0.
25. Lee, K.L.; Hubbard, L.C.; Hern, S.; Yildiz, I.; Gratzl, M.; Steinmetz, N.F.; Author, B.S. Shape Matters: The Diffusion Rates of TMV Rods and CPMV Icosahedrons in a Spheroid Model of Extracellular Matrix Are Distinct NIH Public Access Author Manuscript. *Biomater Sci* **2013**, *1*, doi:10.1039/b000000x/NIH.
26. Yarden, Y.; Pines, G. The ERBB Network: At Last, Cancer Therapy Meets Systems Biology. *Nat. Rev. Cancer* **2012**, *12*, 553–563, doi:10.1038/nrc3309.
27. Hendler, F.J.; Ozanne, B.W. Rapid Publication Human Squamous Cell Lung Cancers Express Increased Epidermal Growth Factor Receptors. *J. Clin. Invest.* **1984**, *74*, 647–651.
28. Sigismund, S.; Avanzato, D.; Lanzetti, L. Emerging Functions of the EGFR in Cancer. *Mol. Oncol.* 2018, *12*, 3–20.
29. Steinmetz, N.F. Viral Nanoparticles as Platforms for Next-Generation Therapeutics and Imaging Devices. *Nanomedicine Nanotechnology, Biol. Med.* 2010, *6*, 634–641.
30. Wen, A.M.; Lee, K.L.; Yildiz, I.; Bruckman, M.A.; Shukla, S.; Steinmetz, N.F. Viral Nanoparticles for in Vivo Tumor Imaging. *J. Vis. Exp.* **2012**, doi:10.3791/4352.
31. Beatty, P.H.; Lewis, J.D. Cowpea Mosaic Virus Nanoparticles for Cancer Imaging and Therapy. *Adv. Drug Deliv. Rev.* **2019**, *145*, 130–144, doi:10.1016/j.addr.2019.04.005.
32. Park, J.; Chariou, P.L.; Steinmetz, N.F. Site-Specific Antibody Conjugation Strategy to Functionalize Virus-Based Nanoparticles. *Bioconjug. Chem.* **2020**, *31*, 1408–1416, doi:10.1021/acs.bioconjchem.0c00118.
33. Martí, M.; Merwaiss, F.; Butković, A.; Daròs, J.A. Production of Potyvirus-Derived Nanoparticles Decorated with a Nanobody in Biofactory Plants. *Front. Bioeng. Biotechnol.* **2022**, *10*, doi:10.3389/fbioe.2022.877363.
34. Sainsbury, F.; Thuenemann, E.C.; Lomonossoff, G.P. PEAQ: Versatile Expression Vectors for Easy and Quick Transient Expression of Heterologous Proteins in Plants. *Plant Biotechnol. J.* **2009**, *7*, 682–693, doi:10.1111/j.1467-7652.2009.00434.x.

 doi:10.20944/preprints202402.0392.v1

35. Sánchez, F.; Ponz, F. Presenting Peptides at the Surface of Potyviruses in Planta. In *Methods in Molecular Biology*; Humana Press Inc., 2018; Vol. 1776, pp. 471–485.
36. Yuste-Calvo, C.; González-Gamboa, I.; Pacios, L.F.; Sánchez, F.; Ponz, F. Structure-Based Multifunctionalization of Flexuous Elongated Viral Nanoparticles. *ACS Omega* **2019**, *4*, 5019–5028, doi:10.1021/acsomega.8b02760.